

Transport model analysis of the transverse momentum and rapidity dependence of pion interferometry at SPS energies

Qingfeng Li ^{1*}, Marcus Bleicher ², Xianglei Zhu ^{1,2,3}, and Horst Stöcker ^{1,2}

1) *Frankfurt Institute for Advanced Studies (FIAS),*

Johann Wolfgang Goethe-Universität, Max-von-Laue-Str. 1,

D-60438 Frankfurt am Main, Germany

2) *Institut für Theoretische Physik,*

Johann Wolfgang Goethe-Universität, Max-von-Laue-Str. 1,

D-60438 Frankfurt am Main, Germany

3) *Physics Department, Tsinghua University, Beijing 100084, P.R. China*

Abstract

Based on the UrQMD transport model, the transverse momentum and the rapidity dependence of the Hanbury-Brown-Twiss (HBT) radii R_L , R_O , R_S as well as the cross term R_{OL} at SPS energies are investigated and compared with the experimental NA49 and CERES data. The rapidity dependence of the R_L , R_O , R_S is weak while the R_{OL} is significantly increased at large rapidities and small transverse momenta. The HBT “life-time” issue (the phenomenon that the calculated $\sqrt{R_O^2 - R_S^2}$ value is larger than the correspondingly extracted experimental data) is also present at SPS energies.

PACS numbers: 25.75.Gz, 25.75.Dw, 24.10.Lx

* E-mail address: liqf@fias.uni-frankfurt.de

The high temperature phase of Quantum Chromodynamics (QCD), i.e., the Quark Gluon Plasma (QGP) has been investigated theoretically and experimentally for many years with energies in \sqrt{s} ranging from around 2 GeV up to 200 GeV. Since the (phase) transition from hadrons to quarks might take place only in a small sub-volume and for a short timespan compared to the overall process of the heavy ion collisions (HICs), it is an intricate but essential task to explore the space-time structure of the region of homogeneity in HICs. Fortunately, a well-established technique called Hanbury-Brown-Twiss interferometry (HBT) [1, 2, 3] has been developed, which is now extensively used in the heavy-ion community to determine the space-time dimensions of the particle emission source for HICs with energies from SIS to RHIC [4, 5, 6, 7, 8, 9, 10, 11, 12, 13, 14, 15, 16, 17, 18, 19, 20, 21, 22, 23, 24, 25, 26, 27, 28, 29, 30, 31, 32, 33, 34, 35]. Studies on various species of two-particles other than identical charged pions have been published or are being pursued (see, e.g. Refs. [4, 24] and the references therein). After more than two decades of progress aiming at relativistic HICs, many basic and important systematic features have been discovered by femtoscopy measurements at SIS, AGS, SPS, and RHIC [4, 16, 23, 24]: the dependence on system size, collision centrality, rapidity, transverse momentum and particle mass (or species).

In our recent work [36], we have investigated theoretically the system size- and the centrality dependence of the HBT radius parameters R_L , R_O , and R_S at RHIC energies. It was found that the calculations are well in line with experimental data, except that the predicted R_O values in central collisions (besides the elementary p+p collisions) are slightly larger than the experimental data. Thus, the R_o/R_s ratio is larger than that extracted from data. This phenomenon is sometimes dubbed the “HBT-puzzle” and reported by most of the other models [4, 26, 27, 37, 38]. In Ref. [41] A Multi-Phase Transport model (AMPT) provides a good fit to data after including a partonic cascade with a certain parton-scattering cross section, while in Ref. [14] the Hadronic Rescattering Model (HRM), which is only based on hadronic rescattering with *instantaneous* collisions, can interpret HBT observables as well. Furthermore, J. G. Cramer et. al. [39] presented one relativistic quantum-mechanical treatment of refractive and opacity effects on two-pion correlations and found a chiral phase transition is required in the dense medium in order to solve the HBT “puzzle” at RHIC, which was further supported by S. Pratt in [40] by considering interactions with mean field in classical trajectories. Ref. [33] argued that the origin of this “HBT- puzzle” might be multifaceted. In this work, we focus our investigation on HICs at lower energies — the

SPS energy regime — partly in order to better understand the origin of the large R_o/R_s in present models. Furthermore, in this energy region, recently the rapidity dependence of the HBT-radii of the pion source was investigated systematically by two experimental collaborations NA49 [35, 42] and CERES [18]. It is expected that the rapidity (or pseudorapidity) dependence of the HBT parameters might provide essential information on the localization of hot and dense nuclear matter and hence it is worthwhile to investigate theoretically.

By using the Ultra-relativistic Quantum Molecular Dynamics (UrQMD, v2.2) transport model (employing hadronic and string degrees of freedom) (for details, the reader is referred to Refs. [43, 44, 45, 46]) and the analyzing program CRAB (v3.0 β) [47, 48, 49] as tools, we compare the calculated transverse momentum and rapidity dependence of HBT-radii with the (preliminary) experimental data at SPS energies [18, 35, 42]. The HBT-radii are represented by using the Bertsch-Pratt three-dimensional convention, which is also called the longitudinal co-moving system or “Out-Side-Long” system. In this work, the three-dimensional correlation function is fit with the standard Gaussian form:

$$C(q_O, q_S, q_L) = 1 + \lambda \exp(-R_L^2 q_L^2 - R_O^2 q_O^2 - R_S^2 q_S^2 - 2R_{OL}^2 q_O q_L), \quad (1)$$

in which q_i and R_i are the components of the pair momentum difference $\mathbf{q} = \mathbf{p}_2 - \mathbf{p}_1$ and the homogeneity length (the HBT-radii) in the i direction, respectively. The λ parameter is the incoherence factor which lies for Bose-Einstein statistics between 0 (complete coherence) and 1 (complete incoherence). Experimentally, the λ parameter is affected by many factors e.g. non-pionic contaminations, (long-lived) resonances, and details of the Coulomb correction. Theoretically, the λ parameter is mainly suppressed by the presence of mediate/long-lived resonances since pions from the decay of these resonances come from a larger source than the directly emitted pions, which results in an overall suppression of the correlation function. The R_{OL} represents the cross-term, which is supposed to vanish at mid-rapidity for symmetric systems. At large rapidities, R_{OL} deviates from zero [50, 51], which will be investigated in this paper as well. In the present UrQMD calculations the potential interactions are not considered (the cascade mode) due to the oppressive computing time. Coulomb final state interactions (FSI) are not taken into account in the program CRAB and the fitting process.

In Figs. 1 and 2 we show the transverse momentum k_T dependence ($\mathbf{k}_T = (\mathbf{p}_{1T} + \mathbf{p}_{2T})/2$) of the HBT- radii R_L (top plots), R_O (middle plots), and R_S (bottom plots) in Pb+Pb reactions at beam energies $E_b = 20, 30, 40, 80$, and 160A GeV, and in Pb+Au reactions at

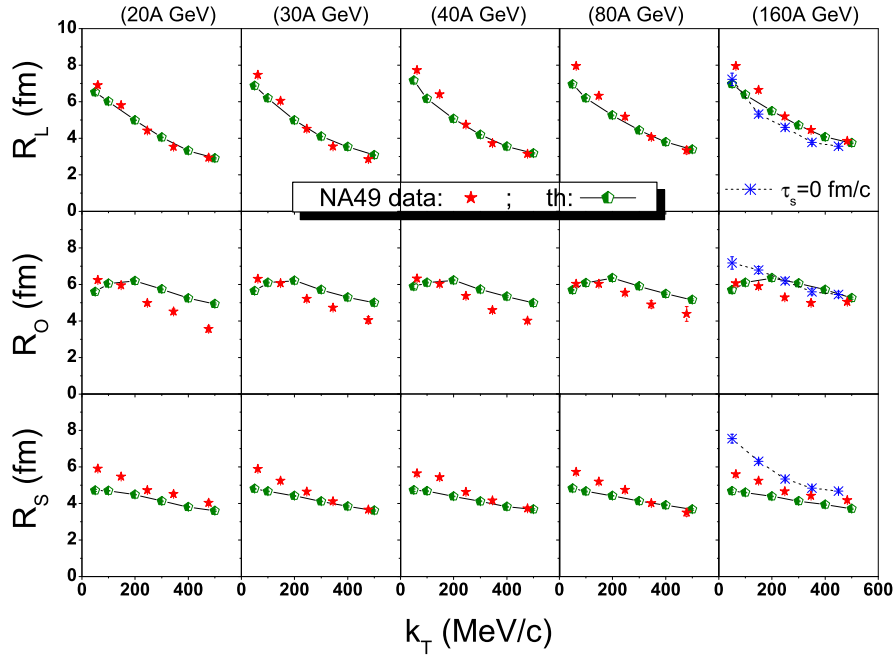


FIG. 1: (Color Online) Transverse momentum k_T dependence of the Pratt-radii in central Pb+Pb collisions at $E_b = 20, 30, 40, 80$, and $160A$ GeV and mid-rapidity $0 < Y_{\pi\pi} < 0.5$. Preliminary NA49 data are taken from [42]. At $E_b = 160A$ GeV the calculation results of the HBT-radii with a vanishing formation time for strings are also presented. As a result, the k_T -dependence of the HBT radii becomes steeper, and the values of R_S are increased and approach the calculated R_O values.

beam energies $E_b = 40, 80$, and $160A$ GeV (plots from left to right), respectively. In Fig. 1 the results are compared with preliminary NA49 data [42] ($< 7.2\%$ of the total cross section σ_T). The pair-rapidity $0 < Y_{\pi\pi} < 0.5$ ($Y_{\pi\pi} = \frac{1}{2}\log(\frac{E_1+E_2+p_{\parallel 1}+p_{\parallel 2}}{E_1+E_2-p_{\parallel 1}-p_{\parallel 2}})$ is the two-pion rapidity with energies E_1 and E_2 and longitudinal momenta $p_{\parallel 1}$ and $p_{\parallel 2}$ in the center-of-mass system) is chosen for all reactions. In Fig. 2, the results are compared with CERES data [18] (the $< 5\%$ most central collisions). The $|Y_{\pi\pi}| < 0.25$ for $40A$ GeV, $-0.5 < Y_{\pi\pi} < 0$ for $80A$ GeV, and $-1.0 < Y_{\pi\pi} < -0.5$ for $160A$ GeV, respectively. Furthermore, the $\pi^- - \pi^-$ correlations are calculated in Fig. 1 while the two-charged-pion correlations (including two- π^- and two- π^+ mesons) are calculated in Fig. 2 (same as experimental outputs). The statistical errors are shown as well. The calculated HBT radii at 160 A GeV by adopting zero formation time

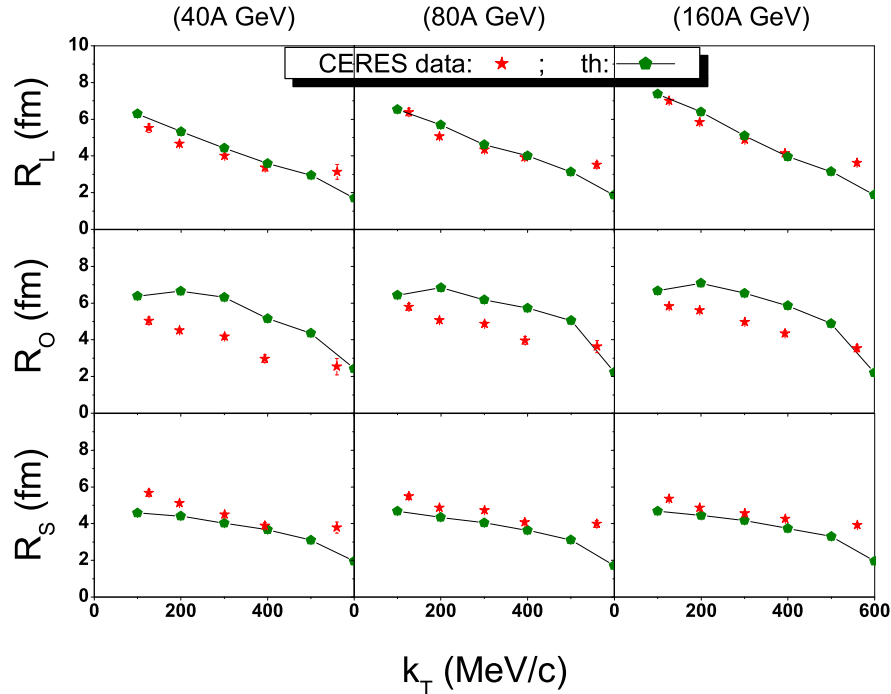


FIG. 2: (Color Online) Transverse momentum dependence of the Pratt-radii in central Pb+Au collisions at $E_b = 40$ ($|Y_{\pi\pi}| < 0.25$), 80 ($-0.5 < Y_{\pi\pi} < 0$), and 160A GeV ($-1.0 < Y_{\pi\pi} < -0.5$). CERES data are taken from [18].

for strings ($\tau_s = 0$ fm/c) will be explained together with Fig. 11. Firstly, it is very interesting to see that the present calculations can reproduce the k_T -dependence of HBT radii R_L and R_S fairly well shown in Figs. 1 and 2. Only at small k_T values, the calculated R_L and R_S values are seen up to 25% lower than data. While for the R_O values, the calculations are shown larger than both NA49 and CERES data especially at relatively large k_T . This deviation appears strongest in most central collisions, which was also seen at RHIC energies [36]. By comparing the NA49 data with the CERES data for central Pb+Pb ($\sigma/\sigma_T < 7.2\%$) and central Pb+Au ($\sigma/\sigma_T < 5\%$) collisions, one observes that the CERES R_O data are somewhat smaller than the recent published NA49 data [42] especially at large k_T and low beam energy $E_b = 40$ A GeV although the recent NA49 data at large k_T have already been driven down visibly when comparing with those preliminary data in the previous publication [35]. The difference between NA49 and CERES data is obviously not due to the differently

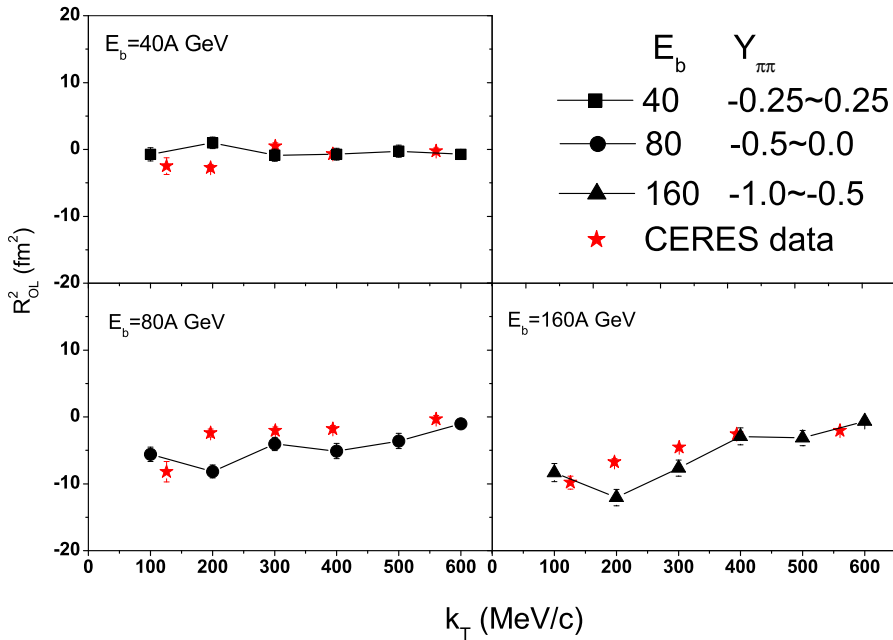


FIG. 3: (Color Online) k_T -dependence of the cross term R_{OL}^2 . Central Pb+Au collisions at $E_b = 40$ ($|Y_{\pi\pi}| < 0.25$), 80 ($-0.5 < Y_{\pi\pi} < 0$), and 160A GeV ($-1.0 < Y_{\pi\pi} < -0.5$) are chosen for comparing with the CERES data taken from [18].

charged pion species since, similar to the HBT results at RHIC [28, 30], we also find that the difference between the HBT-radii of two positively charged and two negatively charged pions is quite small at SPS energies. The origin of these differences between data are still not quite clear.

In addition to the difference between both experimental data in centrality, the selected rapidity cuts are also different in both experiments. The effect of the rapidity-cut on the k_T -dependence of the cross term R_{OL}^2 is shown in Fig. 3 in comparison with the CERES data. In line with the data, an increase of the absolute value of R_{OL}^2 is seen at small k_T with the increase of beam energy. This increase is mainly due to the shift of the rapidity cut away from mid-rapidity with the increase of the beam energy. This effect will also be shown in Figs. 7 and 8. When k_T approaches 0 MeV/c, the value of the cross term R_{OL}^2 also approaches zero, as one expects [51].

Preliminary results on the rapidity dependence of $\pi^-\pi^-$ Bose-Einstein correlations in central Pb+Pb collisions at 20A, 30A, 40A, 80A, and 160A GeV measured by the NA49

collaboration are available [42]. In Figs. 4 and 5 we show the rapidity dependence of the HBT radii R_L (upper plots), R_O (middle plots), and R_S (bottom plots) within two transverse momentum bins: $0 < k_T < 100\text{MeV}/c$ and $100\text{MeV}/c < k_T < 200\text{MeV}/c$, respectively. Here as well as below we only choose three cases with beam energies 20, 40, and 160A GeV as examples. For R_S values shown in Figs. 4 and 5, the R_S of NA49 data decrease with increasing rapidity slowly which is also observed in our calculations despite slightly smaller radii. For R_O results it is seen that the rapidity dependence is weaker than for R_S . The comparison of our calculated results with NA49 data for the rapidity dependence of the R_O values is reasonably well, with the deviation up to 20%. For R_L results, we find a stronger rapidity dependence in the low transverse momentum bin $0 < k_T < 100\text{MeV}/c$ while it is reduced at large momenta. At transverse momenta $0 < k_T < 100\text{MeV}/c$ and at low beam energy $E_b = 20\text{A GeV}$, the R_L value first drops down and then rises again with the increase of rapidity, which is observed as well in our calculations. While at large beam energy 160A GeV a different calculated rapidity dependence of R_L values compared with the preliminary experimental data is found, that is, with the increase of rapidity the calculated R_L value first rises and then drops while the trend of experimental data is still preserved similar to the reactions at lower beam energies although the minimum shifts to a larger rapidity.

As we know, in UrQMD transport model particles are produced via the decay of a meson- or baryon-resonance or by color-strings excitation and fragmentation (the antibaryon-baryon annihilation yields negligible contributions). Keep in mind that the two ways of particle production are different: the former is based on the quasi-particle level (with respect to the resonance masses $m \lesssim 2.5 \text{ GeV}$), while the latter happens at large two-particle center-of-mass energies ($\sqrt{s_{NN}} \gtrsim 2 \text{ GeV}$). Therefore, the string process dominates at the early stage of HICs with large beam energies. While the decay of resonance takes place over the whole evolution of the system. In order to understand the dissimilar rapidity-dependence of R_L at large beam energies, we show in Fig. 6 the single-pion rapidity ($Y_{cm} = \frac{1}{2}\log(\frac{E_1 + p_{\parallel 1}}{E_1 - p_{\parallel 1}})$) distribution of the ratio of the pion numbers at freeze-out from the decay of resonances and strings. Firstly, we see that the mean ratios have exceeded unit which means the decay of resonances dominates at freeze-out and is also of importance to the HBT parameters. In this figure we also find an interesting beam-energy dependence of the ratio as a function of rapidity, e.g., at $E_b = 20\text{A GeV}$, it first drops from mid-rapidity to projectile-target rapidity region and then rises further with increasing rapidity. While at the largest energy point of

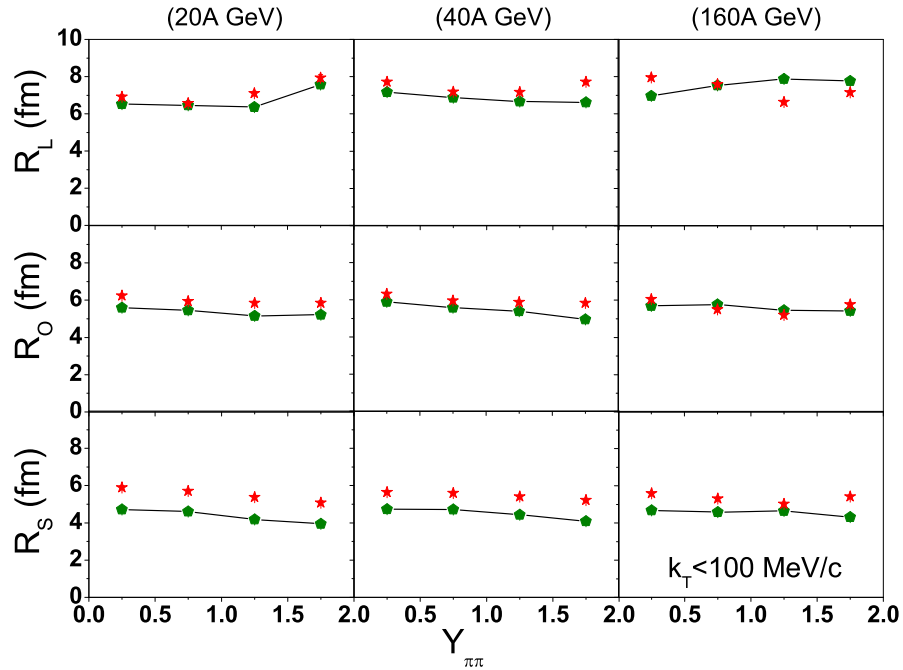


FIG. 4: (Color Online) Rapidity dependence of the HBT-radii R_L (upper plots), R_O (middle plots), and R_S (bottom plots) within transverse momentum bin $0 < k_T < 100\text{MeV}/c$ at beam energies 20, 40, and 160A GeV. The calculations are shown with lines. Preliminary experimental NA49 data are taken from [42] (stars).

SPS, $E_b = 160\text{A GeV}$, the ratio at mid-rapidity is suppressed due that much more pions produced by string fragmentation are treated to transversely emit with small longitudinal velocity. It is known that the case when more pions emitted via the decay of resonance leads to the postpone of pion freeze-out and hence extend the volume of source. While larger fraction of pions via the decay of strings means the freeze-out takes place at earlier stage of overall process and hence a smaller volume of source. Therefore, the cancelation of the two mechanisms of pion freeze-out determines the explicit rapidity dependence of the HBT radii.

Next, we show the rapidity dependence of R_{OL} at transverse momenta $0 < k_T < 100\text{MeV}/c$ (in Fig. 7) and $100\text{MeV}/c < k_T < 200\text{MeV}/c$ (in Fig. 8), in Pb+Pb reactions at 20 (top), 40 (middle), and 160A GeV (bottom). It is seen clearly that the cross term increases with the increase of rapidity which is expected since the longitudinally boost-invariance is

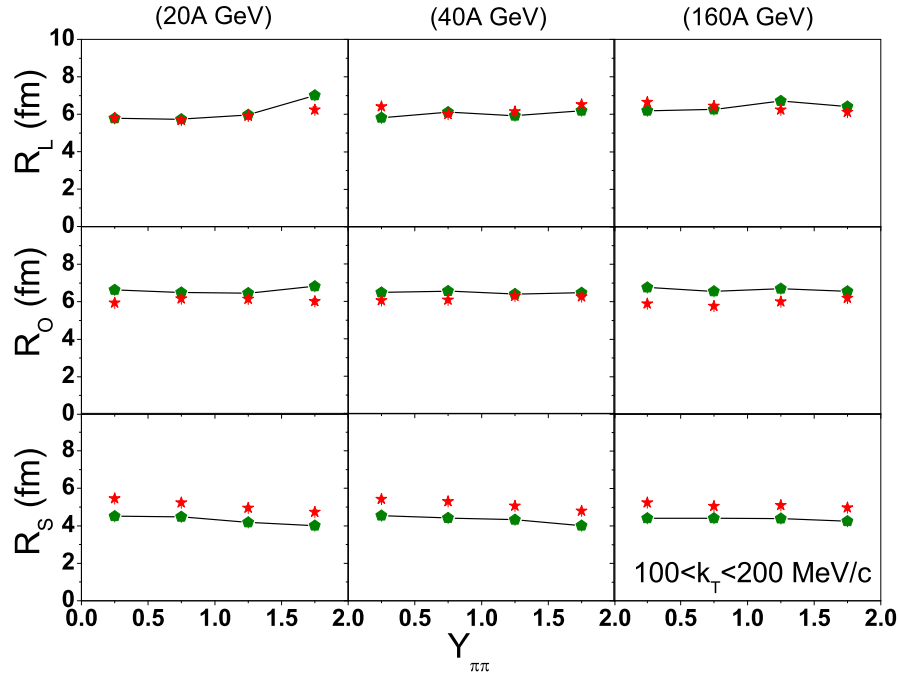


FIG. 5: (Color Online) Rapidity dependence of the HBT-radii R_L (upper plots), R_O (middle plots), and R_S (bottom plots) within transverse momentum bin $100 < k_T < 200 \text{ MeV}/c$ at beam energies 20, 40, and 160A GeV. The calculations are shown with lines. Preliminary experimental NA49 data are taken from [42] (stars).

broken in the forward and backward rapidity regions [51]. We find in our calculations that the inclusion of this cross term modifies the HBT radii R_L , R_O , and R_S only weakly when adopting the rapidity cut $0 < Y_{\pi\pi} < 0.5$. However, it is necessary to include this cross term at large rapidities and small k_T because then it deviates from zero, as shown in Figs. 3, 7, and 8. One also observes that the present calculations reproduce the rapidity dependence of R_{OL} values reasonably well in the rapidity region $0 < Y_{\pi\pi} < 2$.

Figs. 9 and 10 show the rapidity dependence of the quantity $\sqrt{R_O^2 - R_S^2}$ in central $Pb + Pb$ reactions at $0 < k_T < 100 \text{ MeV}/c$ and $100 < k_T < 200 \text{ MeV}/c$, respectively. In certain scenarios [52], the so-called “duration time” $\Delta\tau$ of the pion source is proportional to this quantity at a fixed transverse momentum and has been extensively discussed in the HBT community. However, one should be careful, when interpreting this quantity as “duration time” because this identification only holds in the absence of flow and opacity effects [52].

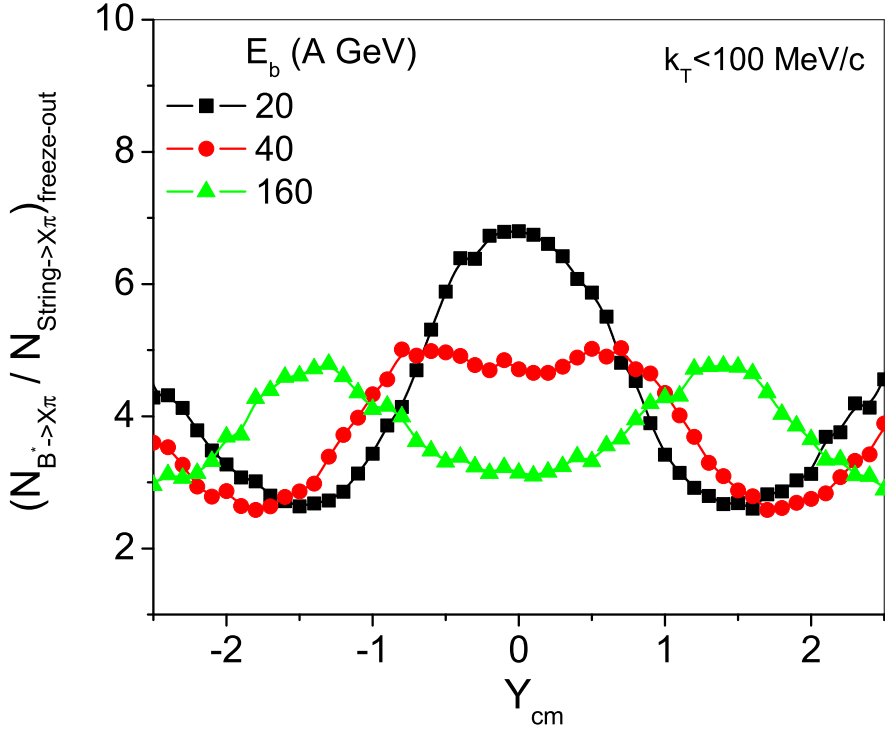


FIG. 6: (Color Online) Single-particle rapidity (Y_{cm}) distribution of the ratio of the pions at freeze-out from the decay of resonances and strings. Three cases at beam energies 20, 40, and 160A GeV are chosen. A similar beam-energy dependence as Fig. 4 in R_L is seen. (see text for details)

Mainly due to a smaller calculated R_S in both transverse momentum bins, the calculated $\sqrt{R_O^2 - R_S^2}$ values are larger than the extracted experimental data at the rapidity interval considered. It is interesting to see that the calculation seems to approach the data at large rapidities $Y_{\pi\pi} = 1.5 \sim 2.0$. In order to solve the HBT ‘‘puzzle’’, the treatment of the interactions during the whole process of HICs should be important. One should notice that the largest deviation of the calculated HBT radii from experimental data comes from the pion correlation at mid-rapidities in the most central collisions, where the interactions are strongest. Owing to the omission of treatment on string-string interactions in UrQMD at early stage, one can argue that the pressure in the early stage might be too small, resulting in a delayed source break-up. The small elliptic flow calculated at RHIC energies is attributed to the same origin [46]. The mean free path of partons (or formation time of particles) from the hot midrapidity region was observed closely linked to the strength of the elliptic flow [53]

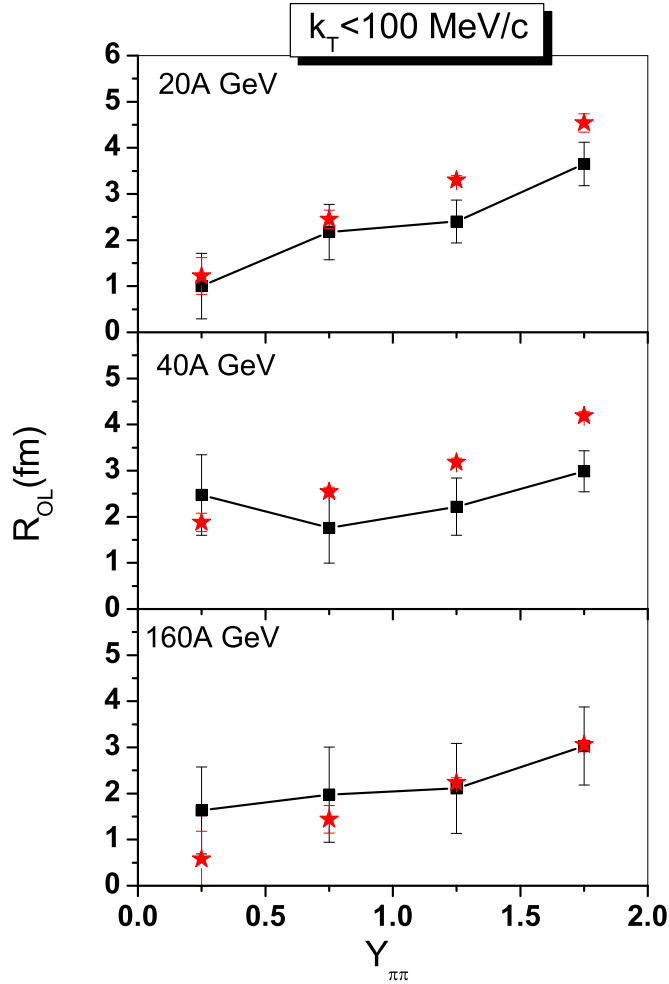


FIG. 7: (Color Online) Rapidity dependence of R_{OL} calculations (lines) at transverse momenta $k_T < 100\text{MeV}/c$ in Pb+Pb reactions at 20 (top), 40 (middle), and 160A GeV (bottom), compared to NA49 preliminary data [42] (stars).

and should also modify the HBT results. In Fig. 1 (in central collisions at $E_b = 160\text{A GeV}$) we show the HBT radii with a zero formation time of particles as well. Due to the reduced mean-free-path of partons and hence much larger transverse pressure at early stage, the k_T fall-off of the HBT-radii is seen even stronger than that found in the data which implies stronger coordinate-momentum correlation in the modified calculations. The R_S rises more strongly than the other two HBT radii and approaches the R_O value. In Fig. 11 the extracted $\sqrt{R_O^2 - R_S^2}$ values from NA49 as well as from CERES data for central collisions as a function of k_T at 160A GeV are compared with calculations of central $Pb + Pb$ collisions with the

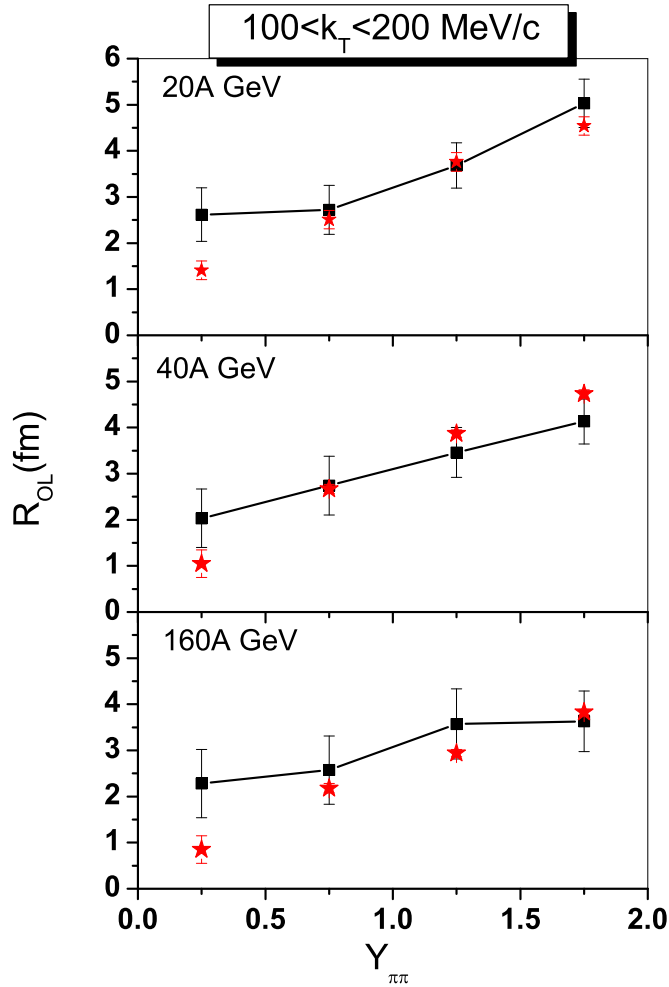


FIG. 8: (Color Online) Rapidity dependence of R_{OL} calculations (lines) at transverse momenta $100\text{MeV}/c < k_T < 200\text{MeV}/c$ in Pb+Pb reactions at 20 (top), 40 (middle), and 160A GeV (bottom), compared to NA49 preliminary data [42] (stars).

default and the reduced formation times of strings. Undoubtedly, the reduced formation time of particles leads to smaller $\sqrt{R_O^2 - R_S^2}$ values. At $k_T < 100\text{MeV}/c$, the calculated R_S values are even larger than R_O values. It is noticed that the CERES R_S data at $k_T \lesssim 500\text{MeV}/c$ are also larger than R_S data. It should be noted that, although a shorter formation time is apt to explain the so-called “HBT-puzzle”, as well the elliptic flow, the absolute values of HBT-radii are not in line with the data (shown in Fig. 1). A more careful treatment on string-string and/or hadron-string interactions as well as the decay of resonances are essential to consistently explain both the single-particle flows and the two-particle correlations.

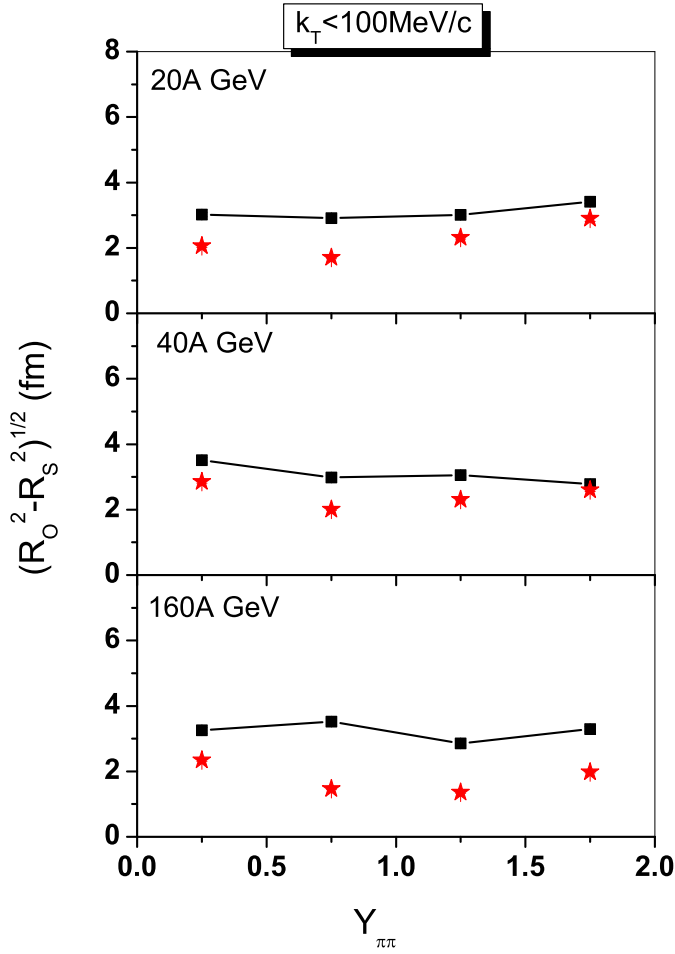


FIG. 9: (Color Online) Rapidity dependence of the calculated quantity $\sqrt{R_O^2 - R_S^2}$ (lines) at $k_T < 100 \text{ MeV}/c$ with beam energies 20 (top), 40 (middle), and 160A GeV (bottom). The preliminary experimental data are illustrated with stars [42].

To summarize, by using the CRAB program, we analyzed the energy and the rapidity dependence of the HBT-parameters R_L , R_O , R_S as well as the cross term R_{OL} at SPS energies in collisions calculated within the UrQMD transport approach. As a whole, the obtained transverse-momentum and rapidity dependences of the HBT-parameters are in reasonable agreement with the experimental NA49 and CERES data, except that the calculated R_O at large k_T and R_S at small k_T are somewhat larger than data. The rapidity dependence of the HBT radii R_L , R_O , R_S is relatively weak while that of the cross term R_{OL} is significant. Comparing our calculations and the experimental data, the so-called “HBT-puzzle” reoccurs at SPS energies —the calculated $\sqrt{R_O^2 - R_S^2}$ values at small k_T are somewhat larger than the

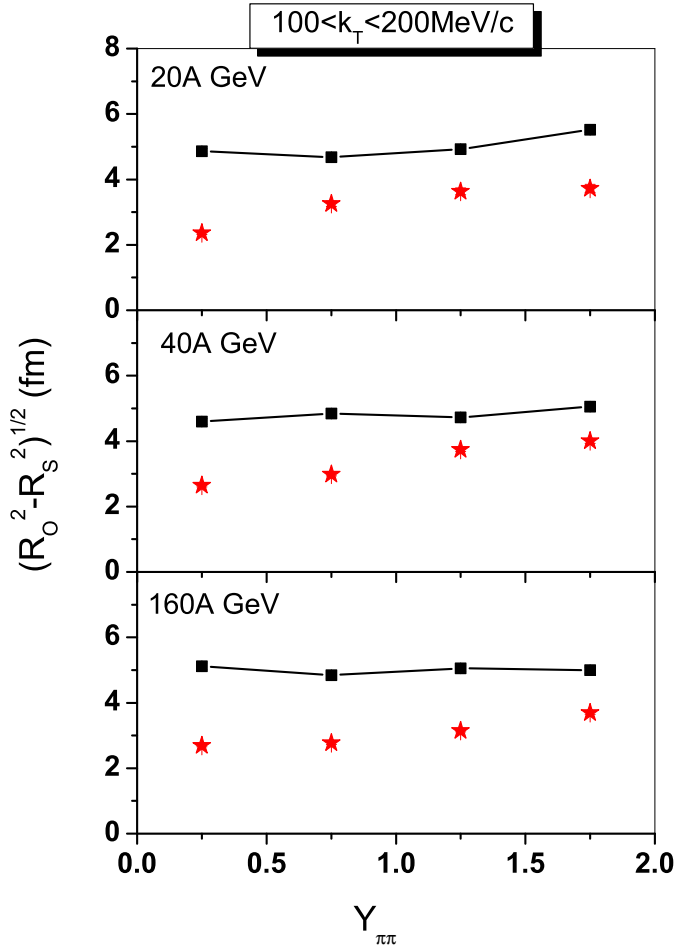


FIG. 10: (Color Online) Rapidity dependence of the calculated quantity $\sqrt{R_O^2 - R_S^2}$ (lines) at $100 < k_T < 200 \text{ MeV}/c$ with beam energies 20 (top), 40 (middle), and 160A GeV (bottom). The preliminary experimental data are illustrated with stars [42].

experimental data. This observation might hint to several open questions in the treatment of the dynamics of HICs, such as the omission of the string-string interactions, the omission of potential interactions of hadrons during the evolution and the involved treatment of resonance production and lifetime in transport models.

Acknowledgments

We would like to thank S. Pratt for providing the CRAB program and acknowledge support by the Frankfurt Center for Scientific Computing (CSC). We thank H. Appelshäuser,

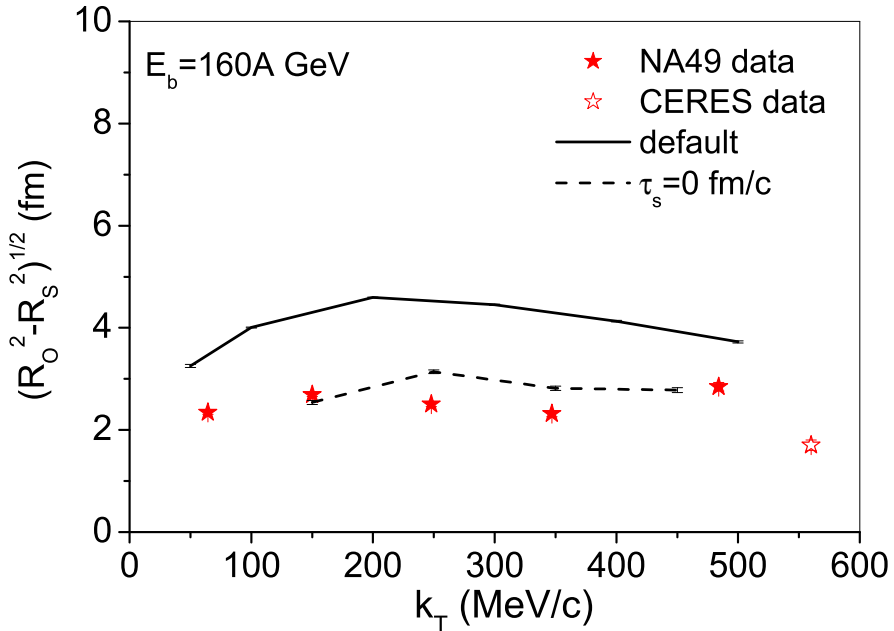


FIG. 11: (Color Online) k_T dependence of the quantity $\sqrt{R_O^2 - R_S^2}$ within $0 < k_T < 100 \text{ MeV}/c$ at beam energy $160A \text{ GeV}$. The default calculation (solid line) and the calculation with a zero formation-time of strings (dashed line) are compared with NA49 data [42] (solid stars) at mid-rapidity as well as CERES data [18] (open stars). The default calculation is somewhat larger than data, which is similar to those in Figs. 9 and 10, while the calculation with reduced formation time matches the measured data on the “duration time”.

M. Gyulassy and T. J. Humanic for helpful discussions and valuable suggestions. Q. Li thanks the Alexander von Humboldt-Stiftung for financial support. This work is partly supported by GSI, BMBF, DFG, and Volkswagenstiftung.

- [1] R. Hanbury-Brown and R.Q. Twiss, *Philos. Mag.* **45**, 663 (1954); *Nature (London)* **178**, 1046 (1956).
- [2] G. Goldhaber, *et al.*, *Phys. Rev.* **120**, 300 (1960).
- [3] W. Bauer, C. K. Gelbke and S. Pratt, *Ann. Rev. Nucl. Part. Sci.* **42** (1992) 77.
- [4] M. A. Lisa, S. Pratt, R. Soltz and U. Wiedemann, *Ann. Rev. Nucl. Part. Sci.* **55**, 357 (2005)
- [5] H. Appelshauser *et al.* [NA49 Collaboration], *Eur. Phys. J. C* **2**, 661 (1998)
- [6] H. Appelshauser *et al.* [NA49 Collaboration], *Nucl. Phys. A* **638**, 91 (1998).
- [7] H. Appelshauser *et al.* [NA49 Collaboration], *Phys. Lett. B* **467**, 21 (1999)
- [8] H. Appelshauser, arXiv:hep-ph/0204159.
- [9] H. Tilsner and H. Appelshauser [CERES Collaboration], *Nucl. Phys. A* **715** (2003) 607.
- [10] H. Appelshauser, *J. Phys. G* **30**, S935 (2004)
- [11] I. G. Bearden *et al.* [the NA44 Collaboration], *Phys. Rev. Lett.* **87**, 112301 (2001)
- [12] D. Peressounko [WA98 Collaboration], arXiv:hep-ph/0403274.
- [13] F. Antinori *et al.* [WA97 Collaboration], *J. Phys. G* **27**, 2325 (2001)
- [14] T. J. Humanic, *Int. J. Mod. Phys. E* **15**, 197 (2006)
- [15] J. Adams *et al.* [STAR Collaboration], *Phys. Rev. Lett.* **93**, 012301 (2004)
- [16] D. Adamova *et al.* [CERES Collaboration], *Phys. Rev. Lett.* **90**, 022301 (2003)
- [17] I. G. Bearden *et al.*, *Phys. Rev. C* **58**, 1656 (1998).
- [18] D. Adamova *et al.* [CERES collaboration], *Nucl. Phys. A* **714**, 124 (2003)
- [19] P. Chung *et al.*, *Phys. Rev. Lett.* **91**, 162301 (2003)
- [20] L. Ahle *et al.* [E802 Collaboration], *Phys. Rev. C* **66**, 054906 (2002)
- [21] P. F. Kolb and U. W. Heinz, arXiv:nucl-th/0305084.
- [22] B. Tomasik and U. A. Wiedemann, arXiv:hep-ph/0210250.
- [23] Z. Chajecki, arXiv:nucl-ex/0511035.
- [24] M. Lisa, arXiv:nucl-ex/0512008.
- [25] S. Soff, S. A. Bass and A. Dumitru, *Phys. Rev. Lett.* **86**, 3981 (2001)
- [26] S. Soff, S. A. Bass, D. H. Hardtke and S. Y. Panitkin, *Phys. Rev. Lett.* **88**, 072301 (2002)
- [27] D. Zschiesche, S. Schramm, H. Stöcker and W. Greiner, *Phys. Rev. C* **65**, 064902 (2002)
- [28] S. S. Adler *et al.* [PHENIX Collaboration], *Phys. Rev. Lett.* **93**, 152302 (2004)

- [29] B. B. Back *et al.* [PHOBOS Collaboration], Phys. Rev. C **73**, 031901 (2006)
- [30] J. Adams *et al.* [STAR Collaboration], Phys. Rev. C **71**, 044906 (2005)
- [31] K. Adcox *et al.* [PHENIX Collaboration], Phys. Rev. Lett. **88**, 192302 (2002)
- [32] U. W. Heinz and P. F. Kolb, arXiv:hep-ph/0204061.
- [33] S. Pratt and D. Schindel, arXiv:nucl-th/0511010.
- [34] M. A. Lisa *et al.* [E895 Collaboration], Phys. Rev. Lett. **84**, 2798 (2000).
- [35] S. Kniege *et al.* [NA49 Collaboration], J. Phys. G **30**, S1073 (2004)
- [36] Q. Li, M. Bleicher, and H. Stöcker, Phys. Rev. C **73**, 064908 (2006).
- [37] D. Molnar and M. Gyulassy, Phys. Rev. Lett. **92**, 052301 (2004)
- [38] T. Hirano and K. Tsuda, Phys. Rev. C **66**, 054905 (2002)
- [39] J. G. Cramer, G. A. Miller, J. M. S. Wu and J. H. S. Yoon, Phys. Rev. Lett. **94**, 102302 (2005)
- [40] S. Pratt, Phys. Rev. C **73**, 024901 (2006)
- [41] Z. Lin, C. M. Ko and S. Pal, Phys. Rev. Lett. **89**, 152301 (2002)
- [42] S. Kniege [NA49 Collaboration], arXiv:nucl-ex/0601024; private communication.
- [43] S. A. Bass *et al.*, [UrQMD-Collaboration], Prog. Part. Nucl. Phys. **41**, 255 (1998).
- [44] M. Bleicher *et al.*, [UrQMD-Collaboration], J. Phys. G: Nucl. Part. Phys. **25**, 1859 (1999).
- [45] E. L. Bratkovskaya, M. Bleicher, M. Reiter, S. Soff, H. Stöcker, M. van Leeuwen, S. A. Bass, W. Cassing, Phys. Rev. C **69**, 054907 (2004).
- [46] X. Zhu, M. Bleicher and H. Stöcker, Phys. Rev. C **72**, 064911 (2005) M. Bleicher *et al.*, in preparation, 2006.
- [47] S. E. Koonin, Phys. Lett. B **70** (1977) 43.
- [48] S. Pratt, CRAB version 3, <http://www.nscl.msu.edu/~pratt/freecodes/crab/home.html>
- [49] S. Pratt *et al.*, Nucl. Phys. A **566** (1994) 103C.
- [50] S. Chapman, P. Scotto and U. W. Heinz, Phys. Rev. Lett. **74**, 4400 (1995)
- [51] U. A. Wiedemann and U. W. Heinz, Phys. Rept. **319**, 145 (1999)
- [52] U. W. Heinz, B. Tomasik, U. A. Wiedemann and Y. F. Wu, Phys. Lett. B **382**, 181 (1996)
- [53] M. Bleicher and H. Stöcker, Phys. Lett. B **526**, 309 (2002)